



Evolution process of luminescent Si nanostructures in annealed SiO_x thin films probed by photoconductivity measurements

Koyanagi, Emi
Uchino, Takashi

(Citation)

Applied Physics Letters, 91(4):041910-041910

(Issue Date)

2007-07

(Resource Type)

journal article

(Version)

Version of Record

(URL)

<https://hdl.handle.net/20.500.14094/90000534>



Evolution process of luminescent Si nanostructures in annealed SiO_x thin films probed by photoconductivity measurements

Emi Koyanagi

Department of Chemistry, Graduate School of Science and Technology, Kobe University,
Kobe 657-8501, Japan

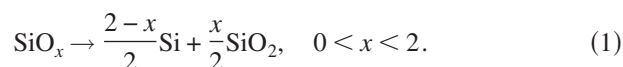
Takashi Uchino^{a)}

Department of Chemistry, Faculty of Science, Kobe University, Kobe 657-8501, Japan

(Received 18 May 2007; accepted 3 July 2007; published online 26 July 2007)

The authors have investigated the photoconductivity (PC) phenomena of SiO_x thin films during annealing, which eventually lead to the formation of luminescent Si nanostructures. It has been found that there are three characteristic annealing stages in the variation of the PC spectral response depending on the microscopic structural transformations of the annealed samples, namely, the elimination of defective midgap states of the as-deposited films, the evolution of conducting Si nanostructures, and the subsequent formation of isolated luminescent Si nanograins. © 2007 American Institute of Physics. [DOI: 10.1063/1.2764441]

For the past decade, Si nanocrystals (NCs) embedded in a SiO₂ matrix have attracted much attention because of their robust photoluminescence (PL) in the visible and near-IR regions, hence providing a promising perspective as Si-compatible optoelectronic devices.^{1–7} One of the often-used methods to fabricate Si NCs/SiO₂ composites is based on the following annealing-induced disproportionation reaction of nonstoichiometric silicon-oxide (SiO_x with $x < 2$) thin films,^{5–7}



It has been well documented that the Si NCs are formed in the SiO_x films by annealing at temperatures $T_a > \sim 1000$ °C, and resulting the PL has been reasonably attributed to the presence of Si NCs.^{5,7,8} However, the underlying mechanism of the dominant radiative recombination process is still under discussion.^{5–10}

Recently, Iacona *et al.*⁸ have demonstrated that SiO_x films annealed at temperatures $T_a < 1200$ °C include amorphous Si nanoclusters and Si NCs, both of which presumably contribute to the observed PL signals.⁸ This implies that it is not crucial for the generation of Si-related PL that the Si nanostructures are crystalline or amorphous.¹¹ In addition, amorphous nanostructures in annealed SiO_x films are interesting since they show rather good electroluminescence (EL) in spite of the inferior PL characteristics.¹² These results imply that there exist compromised optimum Si nanostructures that show the best performance for the respective optical and electrical properties of interest. It is hence interesting to investigate how the dynamics and active roles in optical and electrical processes of carriers created in the Si nanostructures are changed during elevation of annealing temperature. To clarify the issue, we here carry out photoconductivity (PC) measurements of the annealed SiO_x films since PC phenomena such as the photosensitivity, the spectral response, and the time-varying transients are highly influenced by the transport of photoexcited carriers and the resulting recombination mechanisms.¹³

The SiO_x samples used in this study were prepared by electron-beam evaporation of SiO powder (Kojundo Chemical Laboratory Co., Ltd., purity of 99.99%). The films, with a thickness of 500 nm, were deposited on an optical grade silica glass for PC measurements. Silicon substrates were used for Fourier transform infrared (FTIR) spectroscopy and x-ray photoelectron spectroscopy (XPS) measurements. In the vacuum chamber, the background pressure was $\sim 3 \times 10^{-5}$ Pa. The deposition rate was controlled by a quartz microbalance system and was set at 1 nm/s. After deposition, the samples were annealed in an electric furnace with flowing Ar gas at temperatures ranging from 100 to 1100 °C for 2 h. For PC measurements, Au-film interdigital electrodes (ten-pair fingers, 300 μm width, and 100 μm separation) were deposited on the sample, and a monochromated Xe light was used as an excitation source. The intensity of incident light, which is on the order of a few mW/cm², was calibrated according to the spectral response of the optical system. Dark (I_{dark}) and photocurrents (I_{PC}) were measured with a Keithley 6514 electrometer at room temperature under the dc bias voltage of 30 V. No deviation from Ohmic behavior was found for the as-deposited sample for bias voltages up to 35 V. The x values of the silicon oxide phase in the annealed samples were estimated from the empirical relationship between x and peak frequency ν of the infrared absorption band at ~ 1100 cm⁻¹.^{14,15} Si 2p XPS spectra were measured with a Shimadzu ESCA-3400 electron spectrometer equipped with a Mg Kα x-ray source (1253.6 eV). All XPS spectra were corrected using the C 1s peak at a binding energy of 284.4 eV. Time-resolved PL spectra of the annealed samples were observed at room temperature with a gated image intensifier charge coupled device camera and the third harmonic (355 nm) of a nanosecond Nd:YAG (yttrium aluminum garnet) laser (pulse width of 8 ns and average power of 30 mW).

Figure 1 shows the changes in the x values in the silicon oxide phase as a function of the annealing temperature estimated from the FTIR measurements. We see from Fig. 1 that the x values increase with increasing annealing temperature and reach the stoichiometric value at $T_a = \sim 800$ °C. This tendency is in harmony with the XPS spectra shown in the

^{a)}Electronic mail: uchino@kobe-u.ac.jp

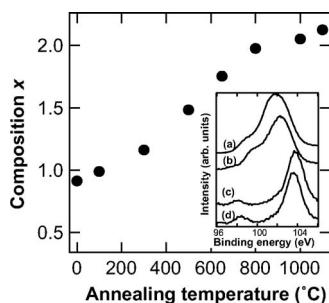


FIG. 1. Composition x of the silicon oxide phase estimated from FTIR measurements for the SiO_x samples as a function of the annealing temperature. The inset shows Si $2p$ peaks in XPS spectra of the (a) as-received, (b) 500 °C, (c) 800 °C, and (d) 1100 °C annealed SiO_x samples.

inset of Fig. 1. The XPS Si $2p$ spectrum of the as-received sample consists of a broad peak centered at ~ 102 eV. After annealing at $T_a = 800$ and 1100 °C, the Si $2p$ signals split into two peaks of ~ 103.5 and ~ 98.5 eV, which are attributed to a SiO_2 phase and a Si phase, respectively.¹⁶ These observations indicate that the present SiO_x films have separated into two more stable SiO_2 and Si phases after annealing at $T_a > \sim 800$ °C according to Eq. (1). It is also interesting to note that we observed a substantial red PL emission only from the samples annealed at temperatures $T_a \geq 1000$ °C (see Fig. 2). We found that the observed PL decay occurs in the time range of microseconds and is characterized by a stretched exponential function: $I(t) = I_0 \exp[-(t/\tau)^\beta]$, where τ is a characteristic decay time and β is a dispersion factor. Since the observed PL behaviors show the typical Si-related PL characteristics of the Si/ SiO_2 nanocomposite,^{8,17–19} it can be concluded that the present high-temperature ($T_a \geq 1000$ °C) annealed samples contain luminescent Si nanostructures.

We next investigate the PC characteristics of the annealed SiO_x films. As for the as-deposited sample and those annealed at $T_a \leq 500$ °C, the observed PC buildup $I_{\text{PCB}}(t)$ is reasonably described by the following double exponential function irrespective of the wavelength of the excitation light [see Fig. 3(a)]: $I_{\text{PCB}}(t) - I_{\text{dark}} = I_{\text{max}} - A_1 \exp(-t/\tau_1) - A_2 \exp(-t/\tau_2)$, where I_{max} is the expected saturated photocurrent and A and τ are fitting constants. Figure 4 shows the

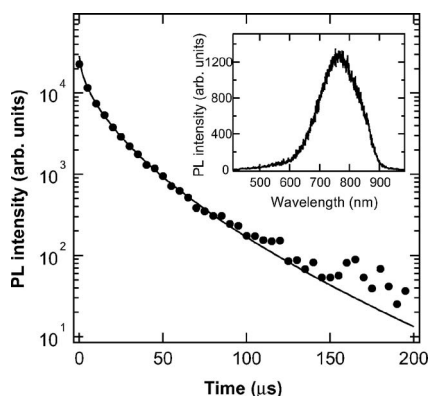


FIG. 2. The photoluminescence decay of the SiO_x sample after annealing at 1100 °C. The PL detection was made at 765 nm. The third harmonic (355 nm) of a pulsed Nd:YAG laser was used for excitation. The experimental data are fitted with a stretched exponential function [Eq. (2)] shown as a solid line. The fitted values of τ and β are $6.0 \mu\text{s}$ and 0.58 , respectively. The inset shows a time-integrated PL spectrum of the same 1100 °C annealed sample. All the measurements were carried out at room temperature.

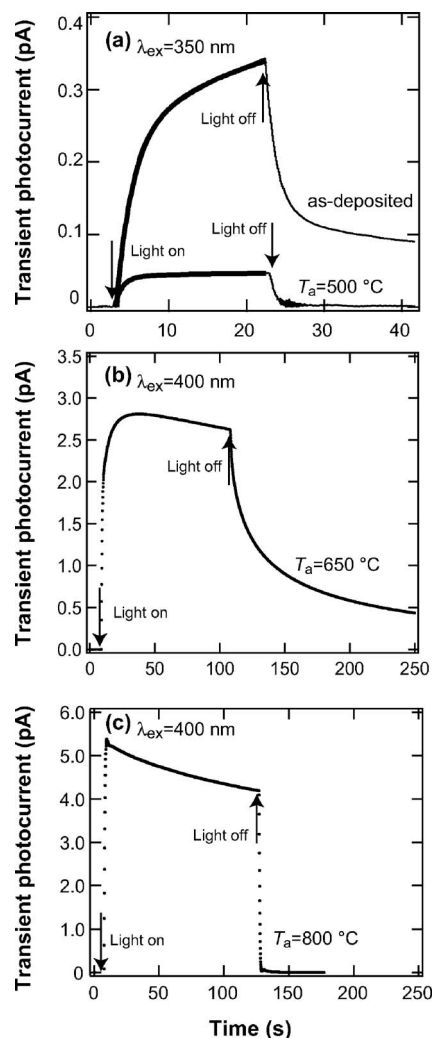


FIG. 3. Examples of transient photocurrent of the (a) as-received and 500 °C, (b) 650 °C, and (c) 800 °C annealed SiO_x samples under the bias of 30 V. A monochromated Xe lamp ($\lambda_{\text{ex}} = 350$ or 400 nm) was used as a light source. The thick solid lines in (a) are least-squares fits with Eq. (3).

values of I_{max} as a function of the excitation wavelength. When the illumination was terminated, there was correspondingly a slowly decreasing current [see also Fig. 3(a)]. These PC buildup and decay behaviors have been generally

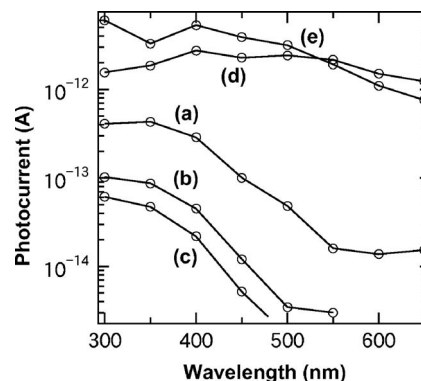


FIG. 4. Photocurrent spectra of the (a) as-received, (b) 300 °C, (c) 500 °C, (d) 650 °C, and (e) 800 °C annealed SiO_x samples under bias of 30 V. As for (a), (b), and (c), the I_{max} values obtained by fitting with Eq. (3) were plotted. As for (d) and (e), the maximum transient photocurrents obtained at the respective excitation wavelengths were plotted. The lines are guides to the eye.

interpreted in terms of carrier trapping in, and releasing from, midgap states.^{20,21} Thus, the time-varying PC phenomena observed for the samples annealed at $T_a \leq 500$ °C most likely originate from the defective midgap states in the as-deposited sample and the related trap-assisted conduction.

When the samples are annealed at 650–800 °C, however, the PC signals show a tremendous increase over the whole range of visible region [see Figs. 3(a), 3(b), and 4]. As mentioned earlier, the disproportionation reaction is almost completed, at least on the macroscopic length scale, in this temperature range. We hence propose that the observed PC gain results from the “silicon” phase in the annealed samples. We also notice from Figs. 3(b) and 3(c) that the transient photocurrent exhibits a gradual decrease even during illumination. Since a similar time-dependent decrease in photocurrent during illumination has been observed from amorphous silicon and chalcogenides but not from the crystalline counterparts,²² we propose that the “amorphous silicon phase” is responsible for the visible PC response from these samples. The above results are in agreement with the previous observations that nanostructured amorphous Si network, instead of isolated clusters, begins to appear in the temperature range from ~ 500 to ~ 900 °C.^{7,8} The sample annealed at 650 °C shows considerable PC transients, similar to the case of the as-deposited sample, whereas the sample annealed at 800 °C shows rather a prompt response to illumination and exhibits virtually no PC transients after the illumination light is switched off. These results imply that the defective trapping centers in and/or around the amorphous silicon phase will be almost annealed out at 800 °C. We also notice from Fig. 4 that the observed photocurrent from the samples annealed at 650 and 800 °C does not simply increase with decreasing the excitation wavelength. This probably results from a redshift of the absorption in the course of the disproportionation reaction and the resulting formation of the amorphous silicon phase. The absorption coefficient of the silicon phase is expected to be quite large in the blue/ultraviolet region as compared with that of the SiO₂ phase. In the high-absorption region, photocarriers are generated only at the near surface, and, accordingly, the relevant photocurrent will not necessarily increase with decreasing the excitation wavelength because of the surface recombination centers.¹³

Finally, we mention the PC characteristics of the samples annealed at $T_a \geq 1000$ °C, from which the Si-related red PL is certainly observed. We found that the dark and photocurrents of the samples annealed at $T_a \geq 1000$ °C were within the noise level (~ 10 fA) under the present experimental condition, indicating that the conductivity decreases by more than three orders of magnitude with increasing annealing temperature from ~ 800 to ~ 1000 °C. This result is in agreement with the results reported by Cooke *et al.*,²³ who showed that the dc conductivity of the SiO_x films annealed at $T_a \geq 1000$ °C is highly suppressed. Thus, in the samples annealed at $T_a \geq 1000$ °C, most of the Si nanostructures are electrically isolated from each other by the surrounding silicon oxide region and the photoexcited carriers will be mainly localized to the respective Si nanostructures, as has also been predicted by the transient terahertz conductivity measurements.²³

As implied earlier, the best annealing conditions for EL does not match with those for PL; a lower temperature an-

nealing is preferred to get a better performance for EL.²⁴ This can be interpreted on the basis of the temperature dependence of the PC mentioned above. Conduction paths, which are prerequisite to an electron injection in the EL process, are present in the samples annealed at lower temperatures ($650 \leq T_a \leq 800$ °C). Such conduction pathways and the related nonradiative recombination centers tend to be eliminated by the higher temperature ($T_a \geq 1000$ °C) annealing, in harmony with the disappearance and appearance of the PC and PL outputs, respectively. We hence believe that the PC measurements are highly informative to characterize the structural transformation process related to the carrier conduction of variously prepared Si/SiO₂ nanocomposites and will be useful to optimize their electronic and optical properties.

In summary, we have shown from the PC measurements that the photoexcited carrier generation and the relevant transport mechanism in SiO_x films are strongly influenced by the degree of disproportionation reaction induced by annealing. The present observations will shed new light on the evolution process of Si nanostructures and their interface states in SiO_x thin films during annealing.

- ¹Y. Kanemitsu, S. Okamoto, M. Otake, and S. Oda, Phys. Rev. B **55**, R7375 (1997).
- ²L. Pavesi, L. Dal Negro, C. Mazzoleni, G. Franzó, and F. Priolo, Nature (London) **408**, 440 (2000).
- ³T. Shimizu-Iwayama, K. Fujita, S. Nakao, K. Saitoh, T. Fujita, and N. Itoh, J. Appl. Phys. **75**, 7779 (1994).
- ⁴T. Inokuma, Y. Wakayama, T. Muramoto, R. Aoki, Y. Kurata, and S. Hasegawa, J. Appl. Phys. **83**, 2228 (1998).
- ⁵F. Iacona, G. Franzó, and C. Spinella, J. Appl. Phys. **87**, 1295 (2000).
- ⁶H. Rinnert, M. Vergnat, G. Marchal, and A. Burneau, Appl. Phys. Lett. **72**, 3157 (1998).
- ⁷D. Nesheva, C. Raptis, A. Perakis, I. Bineva, Z. Aneva, Z. Levi, S. Alexandrova, and H. Hofmeister, J. Appl. Phys. **92**, 4678 (2002).
- ⁸F. Iacona, C. Bongiorno, C. Spinella, S. Boninelli, and F. Priolo, J. Appl. Phys. **95**, 3723 (2004).
- ⁹B. G. Fernandez, M. López, C. García, A. Pérez-Rodríguez, J. R. Morante, C. Bonafos, M. Carrada, and A. Claverie, J. Appl. Phys. **91**, 798 (2002).
- ¹⁰Y. Q. Wang, G. L. Kong, W. D. Chen, H. W. Diao, C. Y. Chen, S. B. Zhang, and X. B. Liao, Appl. Phys. Lett. **81**, 4174 (2002).
- ¹¹G. Allan, C. Delerue, and M. Lannoo, Phys. Rev. Lett. **78**, 3161 (1997).
- ¹²A. Irrera, F. Iacona, I. Crupi, C. D. Presti, G. Franzó, C. Bongiorno, D. Sanfilippo, G. Di Stefano, A. Piana, P. G. Fallica, A. Canino, and F. Priolo, Nanotechnology **17**, 1428 (2006).
- ¹³R. H. Bube, *Photoelectronic Properties of Semiconductors* (Cambridge University Press, Cambridge, 1992), pp. 18–44.
- ¹⁴P. G. Pai, S. S. Chao, Y. Takagi, and G. Lukovsky, J. Vac. Sci. Technol. A **4**, 689 (1986).
- ¹⁵M. Molinari, H. Rinnert, and M. Vergnat, Appl. Phys. Lett. **82**, 3877 (2003).
- ¹⁶X. Y. Chen, Y. F. Lu, L. J. Tang, Y. H. Wu, B. J. Cho, X. J. Xu, J. R. Dong, and W. D. Song, J. Appl. Phys. **97**, 014913 (2005).
- ¹⁷L. Pavesi and M. Ceschini, Phys. Rev. B **48**, 17625 (1993).
- ¹⁸M. Dovrat, Y. Goshen, J. Jedrzejewski, I. Balberg, and A. Sa'ar, Phys. Rev. B **69**, 155311 (2004).
- ¹⁹J. Linnros, N. Lalic, A. Galeckas, and V. Grivickas, J. Appl. Phys. **86**, 6128 (1999).
- ²⁰B. Yan, S. Giralani, and P. C. Taylor, Phys. Rev. B **56**, 10249 (1997).
- ²¹J. Z. Li, J. Y. Lin, H. X. Jing, A. Salvador, A. Botchkarev, and H. Morkoc, Appl. Phys. Lett. **69**, 1474 (1996).
- ²²K. Shimakawa, A. Kolobov, and S. R. Elliott, Adv. Phys. **44**, 475 (1995).
- ²³D. G. Cooke, A. N. MacDonald, A. Hryciw, J. Wang, Q. Li, A. Meldrum, and F. A. Hergmann, Phys. Rev. B **73**, 193311 (2006).
- ²⁴G. Franzó, A. Irrera, E. C. Moreira, M. Miritello, F. Iacona, D. Sanfilippo, G. Di Stefano, P. G. Fallica, and F. Priolo, Appl. Phys. A: Mater. Sci. Process. **74**, 1 (2002).